AN EXPERIMENTAL STUDY OF ROOM-TEMPERATURE RATE-SENSITIVITY, CREEP AND RELAXATION OF AISI TYPE 304 STAINLESS STEEL

E. KREMPL

Department of Mechanical Engineering, Aeronautical Engineering and Mechanics,
Rensselaer Polytechnic Institute, Troy, NY 12181, U.S.A.

ABSTRACT

THE UNIAXIAL viscoplastic behavior of AISI Type 304 stainless steel was investigated by tensile tests at various strain-rates (10^{-8}–10^{-2} s^{-1}), and by short-term creep and relaxation tests up to 5 h. Instantaneous large changes in strain-rate were also performed during monotonic and cyclic loading. A servocontrolled testing machine and displacement measurement on the specimen gage length were used for all tests.

The results show significant rate-sensitivity, creep and relaxation. Test histories involving loading and unloading with positive loads up to 15% strain show that the relaxation behavior in the plastic range depends only on the strain-rate preceding the relaxation test and is independent of the strain magnitude. Also, the relaxation behavior is uniquely related to the stress changes corresponding to instantaneous large changes in the strain-rate during tensile tests. Completely reversed strain-controlled loading gradually changes the stress change/strain-rate change behavior. Annealed specimens and specimens loaded to a cyclic steady-state differ not only in their work-hardening characteristics but also in their rate-dependent behavior. In the cyclic steady-state, different hysteresis loops are traced for different strain-rates with fully reversible transitions from one hysteresis loop to another under strain-rate changes. These results support the notion that the viscoplastic behavior can be represented by piecewise nonlinear viscoelasticity.

1. INTRODUCTION

THE ROOM-TEMPERATURE inelastic deformation behavior of structural metals is generally considered to be rate-independent in yield-surface studies. In "dynamic plasticity", the rate-independent idealization is not always accepted and rate-dependent constitutive equations are frequently used. This difference in viewpoint may be due to the different experimental techniques used in "dynamic" and "static plasticity".

In the first case, "dead load" machines or screw-driven (hydraulically actuated) universal testing machines are employed and the accurate control of the rate-of-load (displacement) application is very difficult. In the latter case, special testing techniques such as the split Hopkinson bar were developed to study the rate-dependent behavior of solids.

The situation has completely changed with the advent of servocontrolled testing equipment which permits accurate control of the rate-of-loading under quasi-static conditions. Such testing machines are frequently employed in fatigue and fracture mechanics testing. However, very little use has been made of them in the

24

determination of stress–strain properties in support of constitutive equation development.

The present study utilizes such equipment for the uniaxial state of stress at room-temperature with the aim of providing experimental support for constitutive equation development. Considerable rate-effects, creep and relaxation are found for annealed AISI Type 304 stainless steel. The results also show that this metal behaves like a nonlinear viscoelastic solid in certain regions of loading.

2. MATERIAL AND SPECIMEN

The test material was AISI Type 304 stainless steel, taken from the "reference heat 9T 2796"† used by the Energy Research and Development Administration, Washington, D.C. Specimens cut from the bar stock were machined to the dimensions shown in Fig. 1. Prior to testing, the specimens were annealed by sealing them in Argon-filled quartz tubes and subjecting the assembly to a temperature of 2000 °F (1093 °C) for 90 min. The stress–strain diagrams of four annealed specimens are shown in Fig. 1. It is seen that the properties are reasonably uniform.

3. TESTING EQUIPMENT AND PROCEDURE

All specimens were tested in an MTS‡ servocontrolled tension–torsion system with dual ramp function generator and the test results were recorded on an *XY* recorder. Displacement was in all cases measured by an MTS clip-on extensometer in the gage length and converted to engineering strain and strain-rate using standard methods. In the following we refer to stress (strain) control, creep and relaxation. In actuality, the load (displacement) is controlled. During creep the load is kept constant, and during relaxation the displacement in the gage length is held fixed.

The clip-on extensometer together with the function generator and the servocontrolled system enable an accurate strain control which is not possible with conventional testing set-ups. By simply changing the command signal, stress control can be achieved in the same test set-up.

We have, basically, two sets of test histories: (i) repeated loading and unloading with no negative stresses and (ii) cyclic, completely reversed strain-controlled histories at an amplitude of 0·4%. Each history is either piecewise linear (ramp forcing function) or consists of creep (constant load forcing function) or relaxation (constant displacement forcing function) intervals. All tests were run at room temperature in air environment.

In some cases the extensometer was rezeroed before the test was restarted. If this is so then the prestrain is noted on the graph. Engineering stresses based on the original cross-section are used throughout. In some graphs we have shown a schematic of the input function to facilitate the interpretation of the results.

In the presentation of the experimental data we first depict typical results under a

---

† Chemical composition (wt %): 0·044 C, 1·26 Mn, 0·033 P, 0·016 S, 0·45 Si, 9·50 Ni, 18·64 Cr, 0·34 Mo, 0·25 Cu.
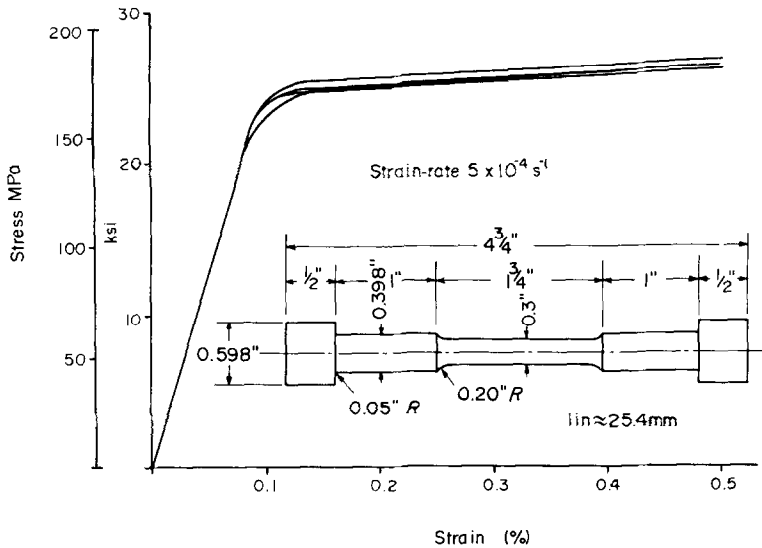
‡ MTS Systems Corporation, Minneapolis, Mi, U.S.A.

FIG. 1. Test specimen and stress–strain diagrams of four annealed specimens.

variety of loading histories. We then report general findings which are pertinent to the "plastic region" (the region where the tangent modulus is small compared to the elastic modulus). These findings are based on the testing of a total of 16 specimens up to a strain level of 15% or more.

4. TEST RESULTS

4.1 *Strain-rate sensitivity*

Figure 2 shows the results of three tensile tests at strain-rates ranging from 10^{-2} to 10^{-8} s^{-1}. In two of the tests the strain-rate was instantaneously changed by three orders of magnitude at points A. Except for the curve with a final strain-rate of 10^{-2} s^{-1}, the slope immediately following the instantaneous change in strain-rate is elastic. The shallow slope for the 10^{-2} s^{-1} curve may be due to the slow response of the XY-recorder. The elastic slope upon a large change in strain-rate was observed in all other strain-rate change tests.

4.2 *Creep*

Figure 3 shows the results of a stress-controlled test at a rate of 283 psi/s (1·95 MPa/s), where the stress was held intermittently constant for 5 min at the points labelled 1, 2, 3, 4, ... The horizontal lines measure the amount of creep occurring during the 5 min period. The creep strain vs time curves are shown in Fig. 4. The accumulated creep strain is increasing with increasing stress and is certainly not negligible at the high stress levels.
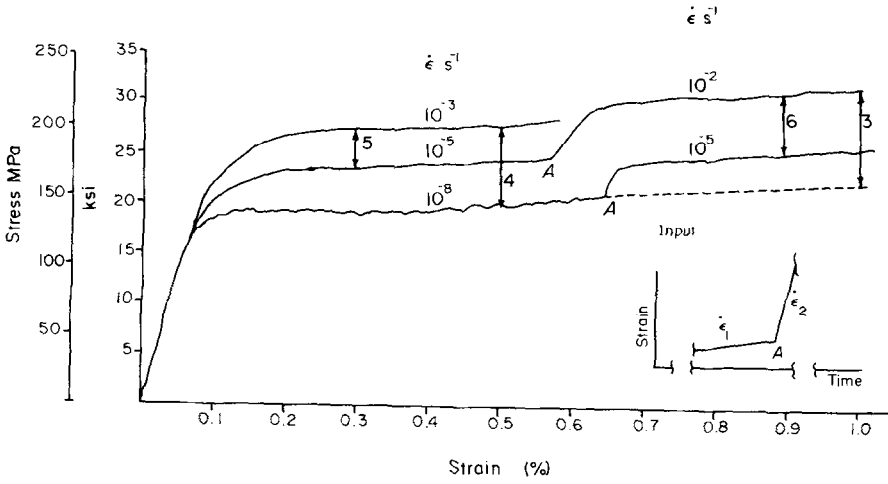
FIG. 2. Stress–strain diagrams at different strain-rates. At points A the strain-rate is instantaneously changed. Annealed AISI Type 304 stainless steel.

4.3 Relaxation

A specimen with prior mechanical history (9% prestrain) involving loading and unloading (but no negative stresses) was first subjected to a strain rate of 10^{-5} s^{-1} with intermittent relaxation periods of 30 s. The vertical bars in Fig. 5 show the amount of stress relaxation during a 30 s interval and demonstrate that relaxation develops gradually and increases with stress increase. Beyond point C the relaxation period commences at points B and lasts for 600 s. Between the relaxation periods the
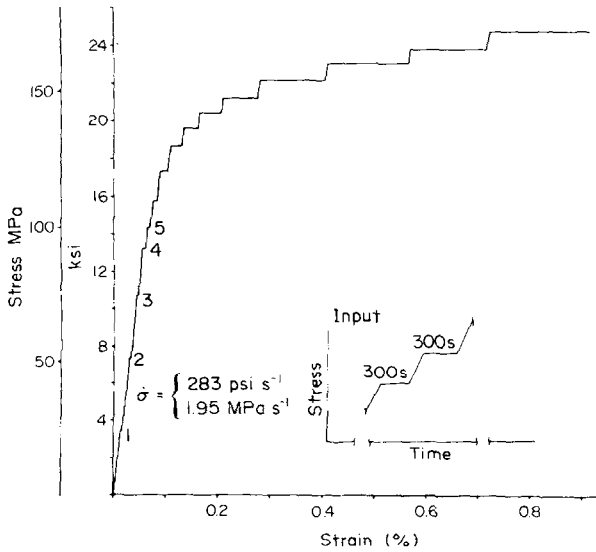

FIG. 3. Stress-controlled loading with intermittent creep periods. Annealed AISI Type 304 stainless steel.
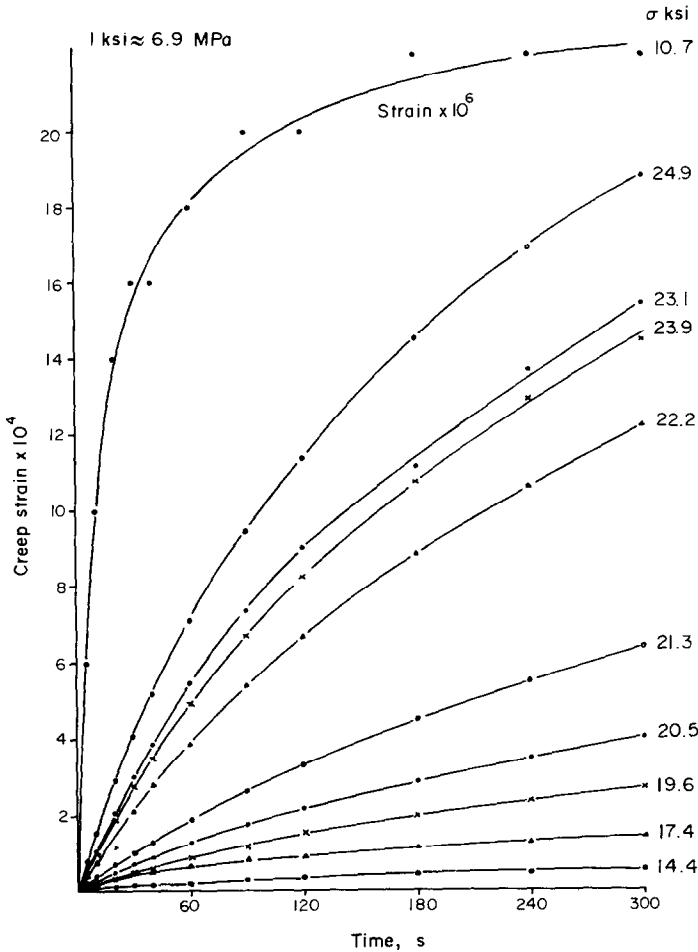
FIG. 4. Creep curves for the tests shown in Fig. 3.

strain-rate is varied between 10^{-6} and 10^{-3} s^{-1}. The data in Fig. 5 clearly show the rate-sensitivity of the material together with significant relaxation. By comparing the total stress change during relaxation in 600 s it is seen that in the plastic region the relaxed stress depends only on the strain-rate of the curve from which relaxation commences.

4.4 Cyclic loading

The behaviour of the material under cyclic loading and repeated strain-rate changes is depicted in Fig. 6. At a strain of $\pm 0.2\%$ the strain-rate was switched between 10^{-3} and 10^{-5} s^{-1}. The ensuing stress changes decrease as the material continues to work-harden.

Ultimately, the material will reach a cyclic steady-state in which the hysteresis loop is traced over, provided the forcing function is not changed. Figure 7 shows the
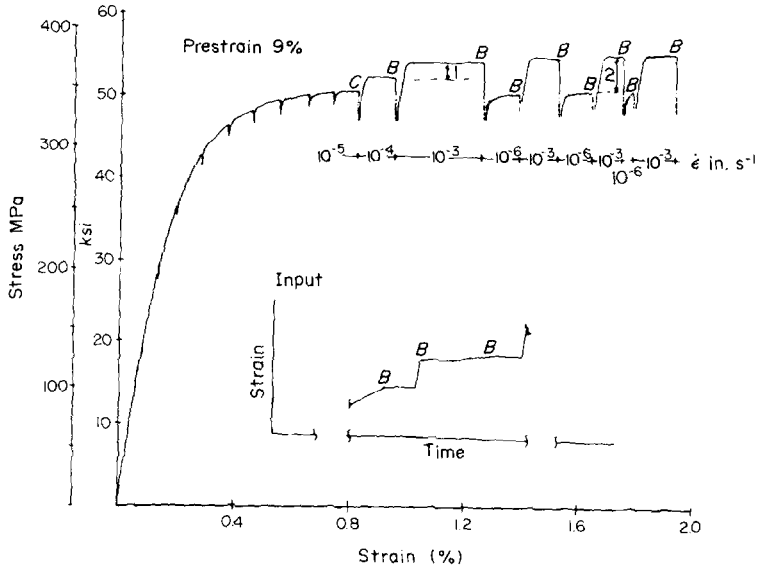
FIG. 5. Relaxation and strain-rate change tests on a prestrained specimen. At points B a relaxation test of
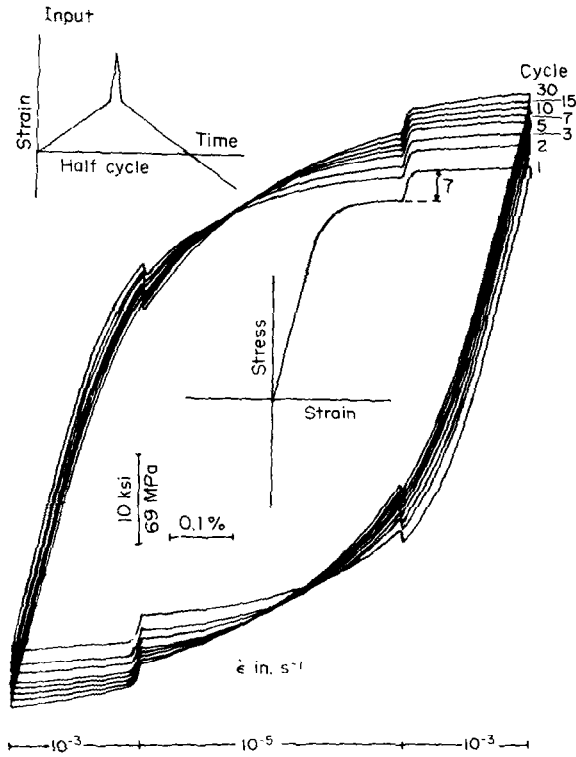600 s duration is started. At strains below point C the relaxation period is 30 s.

FIG. 6. Cyclic straining of an annealed specimen with strain-rate changes at ± 0·2%. The gradual work-
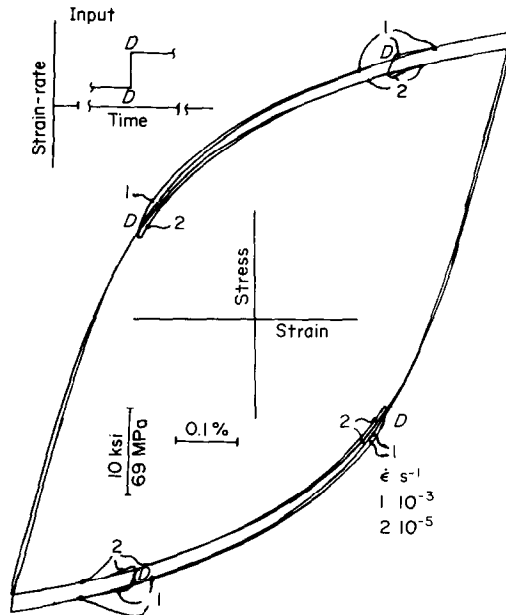hardening and the effects of rate-changes are well developed.

FIG. 7. Steady-state hysteresis loops at strain-rates of 10^{-5} and 10^{-3} s^{-1}. Note that the two loops almost coincide during the unloading portion. At points D the strain-rates were changed. The transition from one to the other hysteresis loop is fully reversible. Continuation of test in Fig. 6.

stabilized hysteresis loop at $\dot{\varepsilon} = 10^{-3}$ s^{-1} (outside curve) and $\dot{\varepsilon} = 10^{-5}$ s^{-1} (inside curve). At $\pm 0.2\%$ the strain-rate was switched between 10^{-3} and 10^{-5} s^{-1}. It is seen that, after an initial overshoot, the hysteresis loops appropriate for the particular strain-rates are reached again.

Figure 8 exhibits the cyclic creep behavior of a specimen with prior mechanical history. Initial loading to point A is followed by cyclic loading between fixed-load limits and subsequent creep for 1 min. After the creep period the load was cycled again at an increased load level. The increasing amount of creep during 1 min with an increase in load and the decrease in accumulated strain/cycle as cycling progresses are apparent.

4.5 Strain-rate changes after cycling

The graph in Fig. 9 depicts the behavior in a tensile test with sudden changes in strain-rate between the values of 10^{-3} and 10^{-5} s^{-1}. Prior to the tensile test the specimen had been subjected to completely reversed cycling at $\pm 0.4\%$ until the cyclic steady-state was reached. Some overshoot consequent upon the changes of strain-rate is apparent which dies out quickly. The steady portions of the curves could be combined to give the stress–strain diagrams at the respective rates.
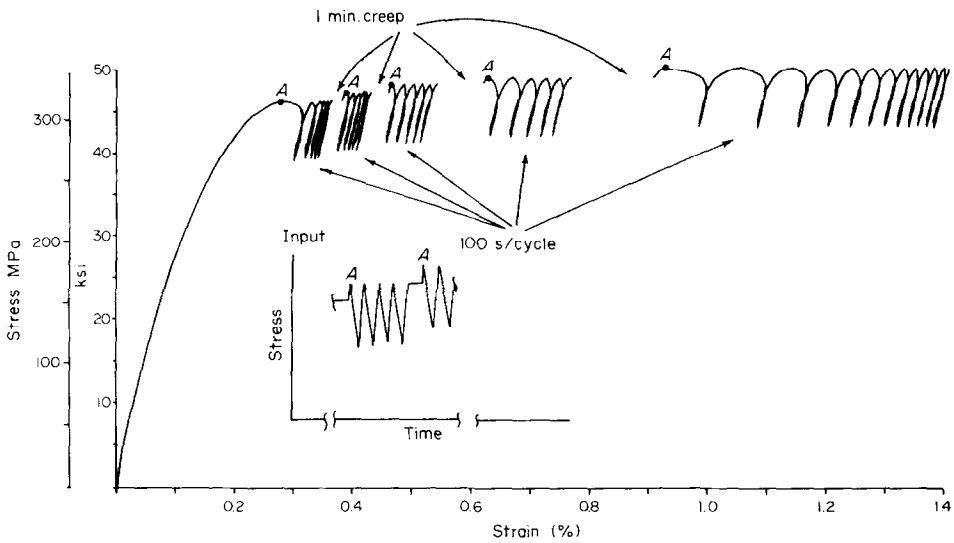
FIG. 8. Cyclic creep of a prestrained specimen. Creep periods of 60 s are followed by load cycling. Note the decrease in "ratchet strain" with cycles.
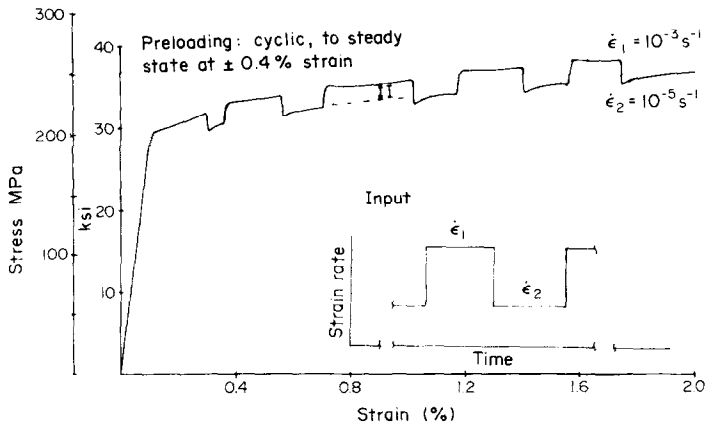

FIG. 9. Response to repeated strain-rate changes in a tensile test. Cyclically prestrained specimen.

5. DATA ANALYSIS AND INTERPRETATION

The copies of actual XY recordings in Figs 2–9 (with the exception of Fig. 4) depict typical behavior of Type AISI 304 stainless steel at room-temperature. The analysis of available additional extensive test data supports the following conclusions.

5.1. *Repeated loading and unloading for positive stresses and strains*

Starting from the annealed condition the material work-hardens considerably; compare the stress levels in Fig. 2 with those in Fig. 5. In the plastic region it was

observed, irrespective of the work-hardened condition, *that the "flow curves" at
various strain-rates are equidistant. The difference $\Delta\Sigma$ between any two curves obtained
at two different strain-rates depends only on the respective strain-rates and is
independent of the actual value of the stress and strain, and there is a nonlinear relation
between $\Delta\Sigma$ and the strain-rates.*

Figure 10 shows $\Delta\Sigma$ (engineering stress†), the stress level difference obtained at
different strain-rates. The stress level corresponding to $\dot{\varepsilon} = 4 \times 10^{-5}$ was taken as the
(arbitrary) zero value. The dots denote data obtained from a specimen repeatedly
loaded and unloaded to zero load between 3 and 9% strain and tested under repeated
strain-rate changes such as shown in Fig. 5.

Also, in Fig. 10 there are large numerals 1–7 which signify stress changes obtained
from Fig. 5 (1, 2), Fig. 2 (3–6) and Fig. 6 (7). The size of these numbers represents
possible scatter. The stress differences 1–7 are plotted assuming that the stress at the
respective largest strain-rate is on the curve traced through the dots.

It is seen that all the points 1–7 coincide with the original curve, within the scatter
of the data. The results shown in Fig. 10 are therefore in support of the statement
given previously.

With regard to the relaxation behavior, in tests started from the points in the
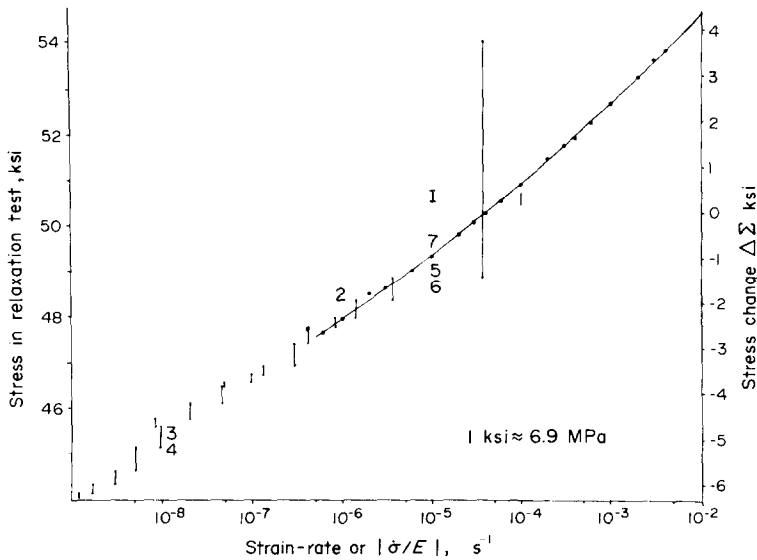plastic region we observed *that in a given time-period the change in relaxation stress*

Fig. 10. Stress change $\Delta\Sigma$ (right scale) vs strain-rate obtained from strain-rate changes in tensile tests and
average inelastic strain-rates vs stress in a relaxation test (left scale). The origin of the right stress-scale is
arranged such that the stress change curve and the relaxation curve overlap. The vertical bars denote
average inelastic strain-rates during a relaxation test. Arabic numerals indicate the stress changes measured
in Figs 2, 5 and 6. I denotes the stress change obtained in the tensile test of Fig. 9. (All the data are plotted
assuming that the stress point at the high strain-rate is on the curve.)

† The use of true stress would change the relation. However, differences between engineering and true
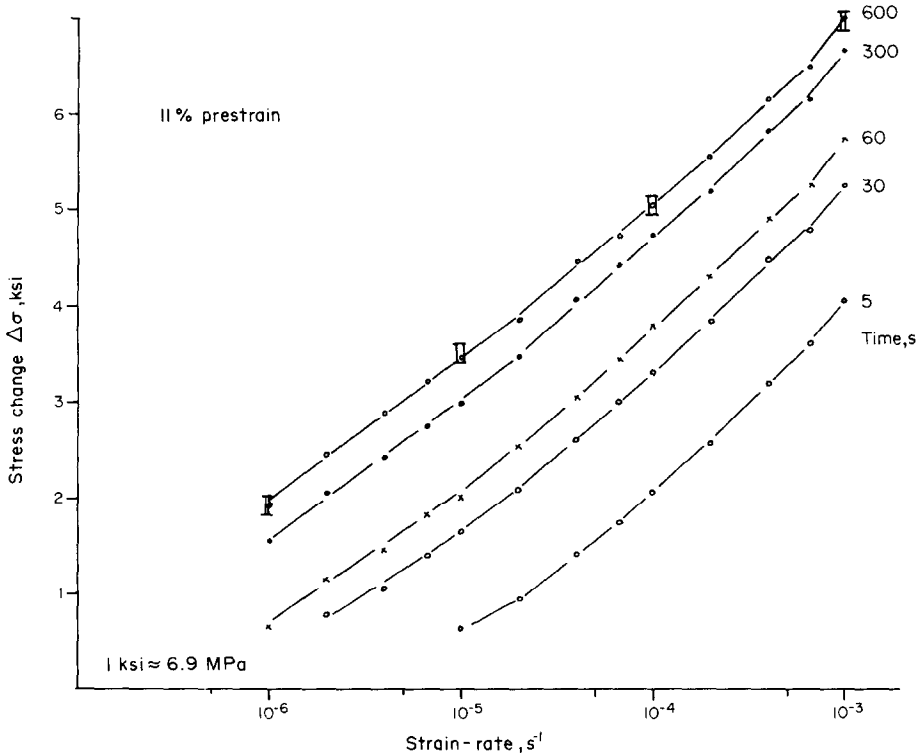stress will not alter the qualitative arguments to be made later.

FIG. 11. Stress change in relaxation tests as a function of the strain-rate of the tensile test preceding the relaxation test. The points labelled II are from Fig. 5.

depends only on the strain-rate preceding the relaxation test and does not depend on the actual value of stress and strain.

In the initial load region, where the slope of the stress–strain diagram is close to the modulus of elasticity, the above statements are not valid. This is partly seen in Fig. 5, where the stress-drop from the curve with $\dot{\varepsilon} = 10^{-5}$ s^{-1} increases with increasing load; compare the relaxation data to the left of point C.

Figure 11 shows the stress relaxation $|\Delta\sigma|$, measured from the start of the relaxation test, at various strain-rates obtained between 11 and 12% strain. The points labelled II are taken from Fig. 5. They match up nicely with the present data. The above statement is also verified by observing that the total change in stress during 600 s is equal for all 4 relaxation tests starting from 10^{-3} s^{-1} in Fig. 5.

The equipment presently available does not allow the accurate determination of the relaxation-rate. It is, however, possible to determine average relaxation-rates by noting the stress at the beginning (σ_i) and the end (σ_e) of an arbitrary time-interval Δt. These data permit the calculation of an average inelastic strain-rate $|\dot{\sigma}/E| = (\sigma_i - \sigma_e)/\Delta t E$. The vertical bars in Fig. 10 show the results. They measure the stress-drop during a given time-interval resulting in the corresponding average inelastic strain-rate. In plotting the relaxation data together with the results of the strain-rate change tests the arbitrary zero-stress level of these tests has been translated

vertically such that the strain-rate change/stress change curve coincides with the relaxation-rate data in the 10^{-6} to 10^{-5} s^{-1} range. It is seen that the relaxation-data are a natural extension of the strain-rate change data.

5.2 Strain-rate changes after cyclic loading to a cyclic steady-state

The previous results demonstrated that the material behavior was reversible, i.e. a certain strain-rate change was associated with a given stress change, irrespective of the actual stress and strain value and the prestrain.

Figure 9 shows the strain-rate change behavior of a specimen with prior cyclic history. The stress change designated by I is plotted in Fig. 10 and falls outside the curve obtained previously for specimens with no reversed loading. We must therefore conclude that cycling to a steady-state condition must have changed the strain-rate change/stress change behavior.

6. DISCUSSION

The experiments reported herein show considerable rate-sensitivity, creep and relaxation of AISI Type 304 stainless steel at room-temperature. They are therefore not in support of the notion of rate (time)-independence of metal deformation at room-temperature. Time-independent plasticity is an inappropriate idealization of this material at room-temperature. Other investigators have also found rate-dependence in AISI Type 304 or 316 stainless steel at room temperature, i.e. the relaxation tests of YAMADA and LI (1973) and THOMAS and YAGGEE (1975); the dynamic tests of ALBERTINI and MONTAGNANI (1976, 1977) and the creep tests by ELLIS, ROBINSON and PUGH (1978, Fig. 3) on AISI Type 316 stainless steel.

Furthermore, the gradual increase of inelasticity shown in Figs 3 and 5 does not support the notion of an abrupt boundary between elastic and inelastic deformation. It rather suggests that inelasticity is a gradually developing process which is initially extremely small but increases with increasing load.

The results of this investigation are in accord with LUBAHN's (1961, p. 325) statement: "We must recognize time-dependence as a basic characteristic of plastic deformation . . .". Also, materials-science oriented studies treat plastic deformation as a rate process (see, for example, KOCKS, ARGON and ASHBY (1975), whose term "plastic deformation" is equivalent to our "inelastic deformation").

The behavior under strain-rate changes in Figs 3 and 10 is reminiscent of the strain-rate history effect reported in studies on dynamic plasticity; see, for example, CAMPBELL and DOWLING (1970), FRANTZ and DUFFY (1972) and KLEPACZKO (1975), to name just a few. However, here we have not observed a strain-rate history effect at all. The flow stress returns to the curve appropriate for the particular strain-rate after an initial overshoot. It should be noted that in the tests reported herein the strain-rate is, within the accuracy of the servocontrol, always equal to the value given on the graphs. Such an accurate control is not possible in the dynamic plasticity tests.

We have only used engineering stress in reporting the data, including Figs 10 and 11. Since prestrains of about 15% are involved, the curves in these figures would be slightly different if true stress had been used. The qualitative features, i.e. stress

changes for sudden changes in the strain-rate are different for cyclically-hardened and monotonically-strained specimens, are not affected by the choice of stress measure.

The difference in the unloading behavior under rate reversal is worth noting. For strain control a very steep positive slope (larger than the elastic modulus) is obtained immediately after strain-rate reversal (see Figs 6, 7 and 9). For load control a small negative slope (much less than the elastic slope) is obtained which gradually changes to a positive slope close to the elastic slope (see Fig. 8). It is clear that the material can "creep" during stress-controlled unloading, whereas no creep is possible during strain-controlled unloading.

The data shown in Figs 10 and 11 suggest that any microstructural changes caused only by tensile loading and unloading have no significant effect on the rate-dependence of the material (specifically the stress change and the relaxation behavior). The effect of plastic deformation is noticeable in the work-hardening of the material; compare the stress levels in Figs 2 and 5. However, the strain-rate change and stress change as well as the relaxation behaviour remain unaffected by monotonic loading or repeated loadings and unloadings involving only positive stresses.

During cyclic straining the work-hardening and the strain-rate change/stress change behavior change (Fig. 6). Once in the cyclic steady-state the material behaves in a fully reversible fashion (see Fig. 7) where the transition between the two loops corresponding to different strain-rates does not cause any further changes in work-hardening or rate-dependence. Tests involving loading histories not exceeding the strain limits of $\pm 0.4\%$ show that the behavior is fully reversible. These tests included cyclic strain-rate changes along the loop, repeated loading and unloading inside the loop and creep and relaxation tests.

This fully reversible behavior in cyclic steady-state entails, compared to the annealed material, an increased work-hardening and a decreased rate-sensitivity (compare Figs 2 and 9).

This result is very significant as it suggests that the effect of deformation-induced microstructural changes is almost exclusively the work-hardening as long as no load reversals are involved. However, cyclic loading causes both work-hardening and a change in the rate-dependence. Evidently, the microstructural changes caused by cyclic loading are different from those induced by monotonic loading. (Indeed it is possible to distinguish monotonically and cyclically loaded specimens by examining their substructure (see NAHM, MOTEFF and DIERCKS, 1977)).

These results are very significant for constitutive equation development. They suggest that there are regions where a metal behaves fully reversibly and according to an equation of state.† The monotonic loading involving no stress reversals as well as the cyclic steady-state are such examples. For monotonic loading only work-hardening and constant rate-dependence must be modelled. However, if cyclic loading is involved then both the work-hardening and the change in rate-dependence must be accounted for. It should be noted that creep, relaxation and rate-sensitivity still have the same form but are changed in "magnitude" after cyclic loading.

A piecewise nonlinear viscoelastic model as proposed by KREMPL (1975) and CERNOCKY and KREMPL (1979a, b) is capable of reproducing this behavior. The

---

† An equation of state is a special form of a constitutive equation; it may depend only on stress, strain and their time derivatives.

changes for cyclic loading are reflected in the updating rules (KREMPL, 1975; LIU, KREMPL and NAIRN, 1976). Indeed, for tensile loading, a good qualitative correspondence between the actual and the numerical experiments is shown by LIU and KREMPL (1979).

REFERENCES

ALBERTINI, C. and   1976   Nucl. Engng Design 37, 115.
  MONTAGNANI, M.   1977   Dynamic Material Properties of Several Steels for
                                   Fast Breeder Reactor Safety Analysis. Rep.
                                   EUR 5787, Euratom-Ispra, Italy.
CAMPBELL, J. D. and   1970   J. Mech. Phys. Solids 18, 43.
  DOWLING, A. R.
CERNOCKY, E. P. and   1979a Int. J. Nonlinear Mech. In press.
  KREMPL, E.   b   Acta Mech. In press.
ELLIS, J. R., ROBINSON, D. N. 1978 Nucl. Engng Design 47, 115.
  and PUGH, C. E.
FRANTZ, R. A. and DUFFY, J. 1972 Trans. ASME 94, Series E, J. appl. Mech. 39, 939.
KLEPACZKO, J.   1975   Mater. Sci. Engng 18, 121.
KREMPL, E.   1975   Acta Mech. 22, 53.
KOCKS, U. F., ARGON, A. S. 1975   Progress in Materials Science 19: Thermodynamics
  and ASHBY, M. F.   and Kinetics of Slip.
LIU, M. C. M., KREMPL, E. 1976   Trans. ASME, Series H, Engng Mater. Tech. 98,
  and NAIRN, D. C.   322.
LIU, M. C. M. and KREMPL, E. 1979   J. Mech. Phys. Solids 27. In press.
LUBAHN, J. D.   1961   Mechanical Behavior of Materials at Elevated
                                   Temperature (edited by J. E. Dorn), p. 325.
                                   McGraw-Hill, New York.
NAHM, H., MOTEFF, J. and   1977   Acta Met. 27, 107.
  DIERCKS, D. R.
THOMAS, J. F. and   1975   Met. Trans. 6A, 1835.
  YAGGEE, F. L.
YAMADA, A. H. and LI, C. Y. 1973   Ibid. 4, 2133.